SECOND EUROPEAN CONFERENCE ON EARTHQUAKE ENGINEERING
AND SEISMOLOGY, ISTANBUL AUG. 25-29, 2014

INVESTIGATION OF SEISMIC VULNERABILITY OF INDUSTRIAL PRESSURE VESSELS

Ioannis MOSCHONAS[1], Christos KARAKOSTAS[2], Vasilios LEKIDIS[3] and Savvas PAPADOPOULOS[4]

ABSTRACT

In the present work a methodology for the derivation of fragility curves for various types of industrial spherical pressure vessels is developed on the basis of static nonlinear (pushover) analysis. Damage states are defined considering only damage developed at the supporting structure and they are quantified using the displacement of the vessel as the damage parameter. The probability density function is idealised as lognormal.

The methodology is applied to two pressure vessels categories, designed without and with braces in their column support system and from the derived pushover curves it is found that the failure of the vessel is caused by the local buckling of critical column sections. Then, the effect of braces on the vessel response is investigated, concluding that bracing increases significantly the stiffness and strength of the overall system, while the stiffeners placed at their connections to columns increase significantly their ultimate ductility. Additionally, the effect of the column section classification on the response of spherical pressure vessels is also investigated.

Finally, representative fragility curves for each pressure vessel category are derived and it is found that braces reduce the fragility of the pressure vessel and provide a significant safety margin against high levels of damage, becoming more effective at progressively higher damage states.

INTRODUCTION

During the last 15 years it became a common practice to assess the seismic vulnerability of a large number of structures, i.e. a 'stock' of structures, through their grouping in structural categories with similar properties and the development of a set of fragility curves for each representative structure category. Until now, the methodology has already been applied successfully to buildings (e.g. FEMA-NIBS, 2010, Lekidis et al., 2005) and to bridges (e.g. FEMA-NIBS, 2010, Karakostas et al., 2006, Moschonas et al., 2009). Regarding industrial structures, the proposed methodologies focus up till now only on storage tanks (FEMA-ASCE, 2001a, b, FEMA-NIBS, 2010).

With regard to spherical pressure vessels Tung and Kiremidjian (1989) proposed three methods for reliability assessment of individual vessels against failure. From their application to a typical spherical pressure vessel with braced lateral load resisting system, it was found that its reliability is increased by strengthening of the structural components that initiate the possible failure mechanisms. Twenty two years later Curadelli (2011) investigated the improvement of the seismic performance of pressure vessels using energy dissipation through seismic risk analysis, concluding that the use of

[1] Civil Engineer, MSc, PhD, Consulting Engineer, Katerini- Greece, jfmoschon@kat.forthnet.gr
[2] Research Director, EPPO-ITSAK, Thessaloniki - Greece, christos@itsak.gr
[3] Research Director, EPPO-ITSAK, Thessaloniki - Greece, lekidis@itsak.gr
[4] Civil Engineer, MSc, PhD Candidate, Aristotle University of Thessaloniki, Greece, savvaspp@civil.auth.gr

energy dissipation devices may reduce the seismic risk and the seismic fragility against failure by 85% and 111%, respectively.

In the framework of an ongoing, EU/Greece co-financed research program on risk assessment of industrial facilities (see Acknowledgements), a methodology for the derivation of fragility curves for spherical pressure vessel stocks has been developed. At first, pressure vessels are classified on the basis of the major parameters that affect their seismic response. Then, an analytical approach is developed for the derivation of fragility curves, which is based on static nonlinear (pushover) analysis. Damage states are defined on the bilinearly idealised pushover curve using the vessel displacement as damage parameter and taking into account only damage developed at the pressure vessel structure, and not to any attached equipment or piping system.

CLASSIFICATION OF SPHERICAL PRESSURE VESSELS

The main parts of a spherical pressure vessel are the spherical shell, wherein the pressurised liquid is stored and the supporting structure, which consists of columns with or without braces. In typical design practice the seismic force is carried by the supporting structure; thus, depending on the type of their lateral load resisting system (LLRS) spherical pressure vessels are classified into the following two categories:

a) With moment-resisting LLRS (i.e. without braces)
b) With braced LLRS

In the first category, the lateral load resisting system consists only of columns, while in the second consists also of usually diagonal braces, concentrically connected to the columns. As a rule, the shell of the pressure vessel is designed to remain in the elastic range during the earthquake. Consequently, the seismic input energy is absorbed in both categories at the LLRS by the formation of plastic hinges at critical column sections, i.e. at the top, below their connections to the shell, and/or at their base, and additionally, in the second category, by yielding of the braces.

METHODOLOGY FOR THE DERIVATION OF FRAGILITY CURVES

The proposed methodology is based on static nonlinear (pushover) analysis, given that damage states are defined on the bilinearly idealised pushover curve of the pressure vessel. This basic idea was previously applied to bridges by Moschonas et al. (2009) for earthquakes that act along a bridge's principal directions and it was further extended for arbitrary angle of incidence of the seismic action by Moschonas and Kappos (2011). The adaption and extension of the methodology for the case of spherical pressure vessels is described in detail in the following sections.

DERIVATION OF PUSHOVER CURVES

Spherical pressure vessels have two modes of vibration, due to their symmetry: one translational and one torsional. Thus, pushover curves are derived by performing a pushover analysis with force distribution compatible with the translational mode (standard pushover analysis). Typical pushover curves for each of the two categories of spherical pressure vessels are shown in Fig. 1.

In the case of vessels with moment-resisting LLRS (Fig. 1a) the first branch of the pushover curve is elastic up to the first yield, which takes place at a critical column section. As the seismic load increases, successive column failures due to buckling take place up to the ultimate point (denoted with the subscript 'u'), after which the vessel becomes unstable.

In the case of vessels with braced LLRS (Fig. 1b) the first branch of a typical pushover curve is also elastic up to the first yield, which in this case is usually caused by the yield of the braces that are parallel -or almost parallel- to the loading direction. The increase of the seismic load leads to successive buckling failures of the columns until the vessel becomes unstable after the ultimate point. Up to this point, braces have not yet reached their ultimate deformation, ε_u. It is noted that Eurocode 3 (EC3, CEN/TC250/SC3, EN 1993-1-1, 2005) classifies cylindrical column sections in 3 classes, in

relation to the diameter-to-thickness ratio. According to this classification, the buckling failure of a column is expected to be caused by local buckling of critical sections for class 2 and 3 sections and by global buckling of the column for class 1 sections.

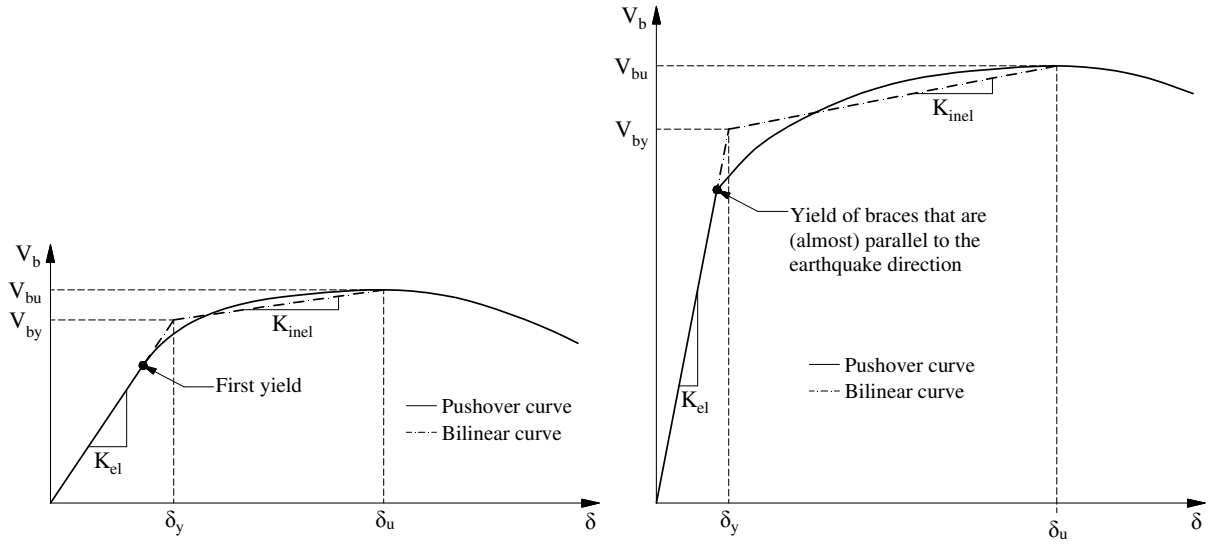

a. Moment-resisting LLRS b. Braced LLRS

Figure 1. Typical pushover curves of spherical pressure vessels

The derived pushover curve is then idealised as bilinear up to its ultimate point (forcing the initial branch of the bilinear curve to have the same slope as the elastic branch of the pushover curve) by equalising the areas between the two curves in order to define the conventional yield point (denoted with the subscript 'y' in Fig. 1).

DEFINITION OF DAMAGE STATES

For the needs of the present research effort, four damage states in addition to the No Damage state (DS0) are defined: Minor/Slight Damage (DS1), Moderate Damage (DS2), Major/Extensive Damage (DS3) and Failure/Collapse (DS4). At first, the thresholds for the four damage states are defined qualitatively describing for each one the corresponding damage developed at the supporting structure of the pressure vessel.

DS1 – Minor/Slight Damage: Minor yields that correspond to minor permanent deformations at critical sections of a small percentage of columns and/or braces.

DS2 – Moderate Damage: For class 1 sections according to EC3, moderate yields corresponding to moderate permanent deformations at critical sections of a moderate percentage of columns and/or braces without any global buckling failure of columns. For class 2 and 3 sections according to EC3, minor-to-moderate yields that correspond to minor-to-moderate permanent deformations at critical sections of a moderate percentage of columns and/or braces without any local buckling at critical sections of columns.

DS3 – Major/Extensive Damage: For class 1 sections according to EC3, major yields causing major permanent deformations at critical sections of a large percentage of columns and/or braces with global buckling failure of columns where maximum compression occurs. For class 2 and 3 sections according to EC3, minor-to-major yields that cause minor-to-major permanent deformations at critical sections of a large percentage of columns and/or braces with local buckling of critical sections at the columns where maximum compression occurs.

DS4 – Failure/Collapse: Buckling failure with subsequent collapse of the pressure vessel.

After the qualitative definition, damage states are quantified in the present research effort by using the displacement δ_{PV} of the control point (top of the vessel shell in our case) as global damage parameter at characteristic points of the bilinearly idealised pushover curve. The proposed threshold values δ_{DSi} of the vessel displacement for each damage state are given in Table 1.

Table 1. Damage state threshold values δ_{DSi} of vessel control point displacement δ_{PV}

Damage State	Threshold value δ_{DSi}
DS1: Minor/Slight Damage	$> 0.9 \cdot \delta_y$
DS2: Moderate Damage	$> \delta_y + (1/3) \cdot (\delta_u - \delta_y)$
DS3: Major/Extensive Damage	$> \delta_y + (2/3) \cdot (\delta_u - \delta_y)$
DS4: Failure/Collapse	$> \delta_u$

DERIVATION OF FRAGILITY CURVES

The derivation of fragility curves starts with the quantification of the exceedance of a certain damage state in terms of the selected global damage parameter, i.e. the vessel top displacement δ_{PV}. As earthquake intensity parameter the peak ground acceleration, A_g, is selected.

The available capacity of the pressure vessel which corresponds to the damage state DSi (i=1 to 4) is quantified through the corresponding threshold value of the vessel displacement δ_{DSi} (Table 1). The response of the pressure vessel for a given earthquake intensity level A_g is quantified through the vessel displacement $\delta_{PV|Ag}$, calculated from the analysis of the pressure vessel for earthquake intensity A_g. So, the exceedance of a certain damage state can be expressed as

$$\delta_{PV|Ag} \geq \delta_{DSi} \tag{1}$$

and the probability of exceedance can be written as

$$P\left(\delta_{PV|Ag} \geq \delta_{DSi}\right) = P_f \tag{2}$$

The next step is the quantification of the total uncertainty which mainly stems from corresponding uncertainties on the seismic demand, the structural capacity and the definition of damage states. In the present study, the probability density function is idealised as lognormal; thus, the total uncertainty is represented by the lognormal standard deviation, β_{tot}, and the probability of exceedance is written as

$$P_f = \Phi\left[\frac{1}{\beta_{tot}} \cdot \ln\left(\frac{\delta_{PV|Ag}}{\delta_{DSi,m}}\right)\right] \tag{3}$$

where $\Phi(\cdot)$ is the standard normal cumulative distribution function and $\delta_{DSi,m}$ is the median threshold value of vessel control point displacement for damage state DSi, which coincides with the corresponding threshold value δ_{DSi} defined in Table 1. Due to lack of previous studies regarding the estimation of the total uncertainty for the case of spherical pressure vessels, β_{tot} is estimated utilising the values given in the literature for elevated steel tanks. More specifically, in American Lifelines Alliance (FEMA-ASCE, 2001a) a value of 0.55 is suggested and it is the average of the corresponding values (0.50 for DS1/ DS2 and 0.60 for DS3/ DS4) suggested in HAZUS (FEMA-NIBS, 2010); thus, in the present research effort the total uncertainty is set to β_{tot}=0.55, as well. The next step is to express the probability of exceedance as a function of the earthquake intensity parameter, A_g. For this reason A_g is correlated with δ_{PV} through the median damage evolution curve (or primary vulnerability curve, Fig. 2), which is the plot of vessel displacement for increasing earthquake intensity levels versus the corresponding peak ground acceleration, A_g.

Hence, the probability of exceedance can now be estimated by the following expression

$$P_f = \Phi\left[\frac{1}{\beta_{tot}} \cdot \ln\left(\frac{A_g}{A_{g,DSi,m}}\right)\right] \tag{4}$$

and its plot is the fragility (probabilistic vulnerability) curve (Fig. 2) of the specific damage state.

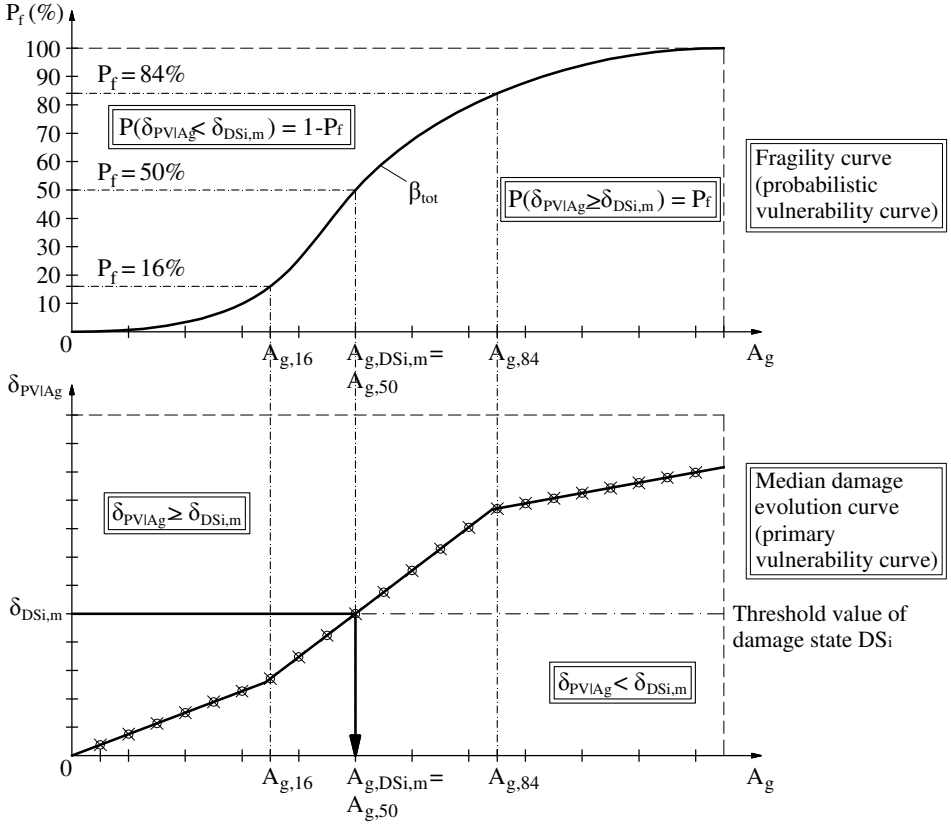

Figure 2. Median damage evolution (primary vulnerability) curve and fragility (probabilistic vulnerability) curve

APPLICATION TO SPHERICAL PRESSURE VESSELS

DESCRIPTION AND MODELLING OF THE SELECTED VESSELS

For the application of the proposed methodology two spherical pressure vessels were investigated; one with moment-resisting LLRS (PV1, Fig. 3a) and one with braced LLRS (PV2, Fig. 3b). The properties of these vessels are summarised in Table 2. It is noted that PV2 is considered as fully filled, i.e. with k_f=100%, so as to ignore the effect of the filling level on its response. The column-height to shell-diameter ratio (H/D) of the investigated structures is in the range of 0.60 ÷ 0.70 (see Table 2), which is commonly met in industrial facilities.

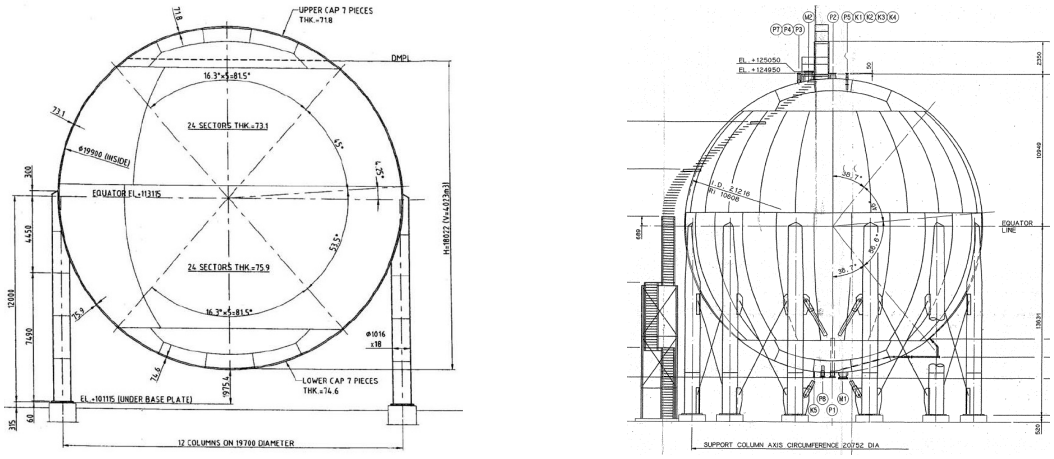

a. PV1 (Moment-resisting LLRS) b. PV2 (Braced LLRS)

Figure 3. Selected spherical pressure vessels

Table 2. Properties of the investigated pressure vessels

Parameter	PV1	PV2
Mean diameter of the shell, D	19.900 m	20.216m
Average shell thickness, t_s	74.5 mm	42 mm
Height to equator, H	12.000 m	13.631 m
Height to shell diameter ratio, H/D	0.603	0.674
Number of columns, N	12	12
Column cross section	CHS 1016×18	From CHS 1100×25-30 up to 3.035 m from the base to CHS 1100×25 at the rest column height
Section class (EC3)	3	2
Steel grade of shell	SA 537-M Class 2	SA 516 Gr. 70
Steel grade of columns	SA 572 Gr. 50 (S355JR)	SA 572 Gr. 50 (S355JR)
Braces cross section	----------	PL 250×35
Steel grade of braces	----------	SA 738 Gr. B
Liquid density, ρ_L	0.522 t/m^3	0.553 t/m^3
Filling level, k_f	100%	90%
Internal pressure, p_i	24 bar	11.2 bar
Foundation supports	Pinned	Pinned

Both vessels are analysed using ABAQUS software. In both vessels (Fig. 4) shell and columns are modelled using shell elements with reduced integration capability (S4R) in a symmetric mesh following the radial symmetry of the vessels. Regarding diagonal braces in PV2 (Fig. 4b) only those in tension are modelled using truss elements, since those in compression are not considered due to their negligible compressive strength due to buckling. Geometric and material nonlinearities are also considered; the former by considering large displacements and strains and the latter by utilising a bilinear model for steel with isotropic hardening.

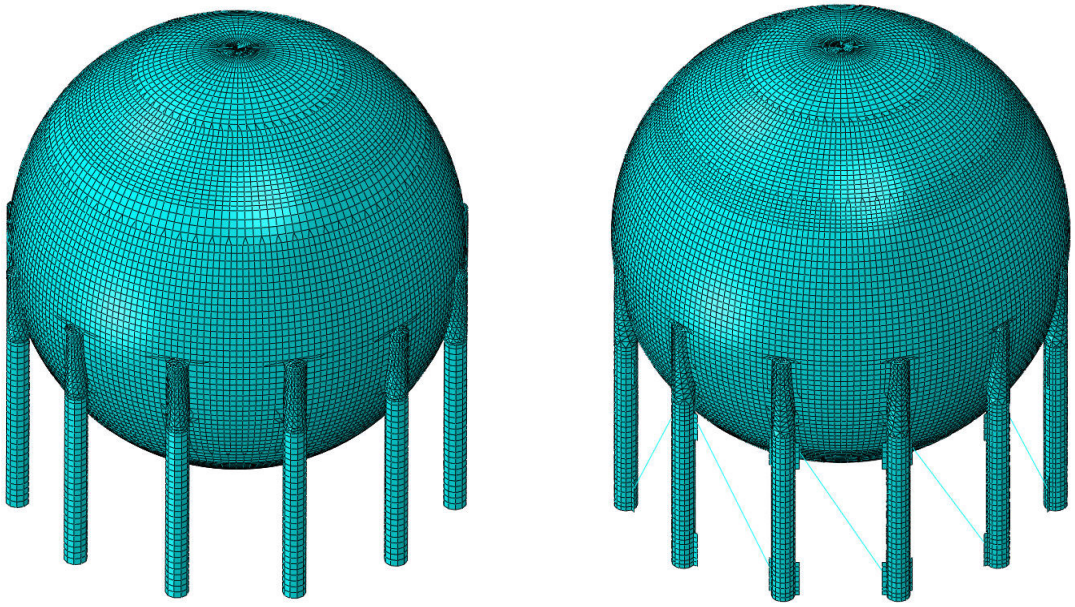

a. PV1 (Moment-resisting LLRS) b. PV2 (Braced LLRS)

Figure 4. Finite element models of the selected spherical pressure vessels

APPLICATION OF THE PROPOSED METHODOLOGY

Having selected and modelled the two spherical pressure vessels the proposed methodology is then applied. At first, the pushover curves of these two vessels (as built case hereafter denoted by ‘AB’) were derived (Fig. 5).

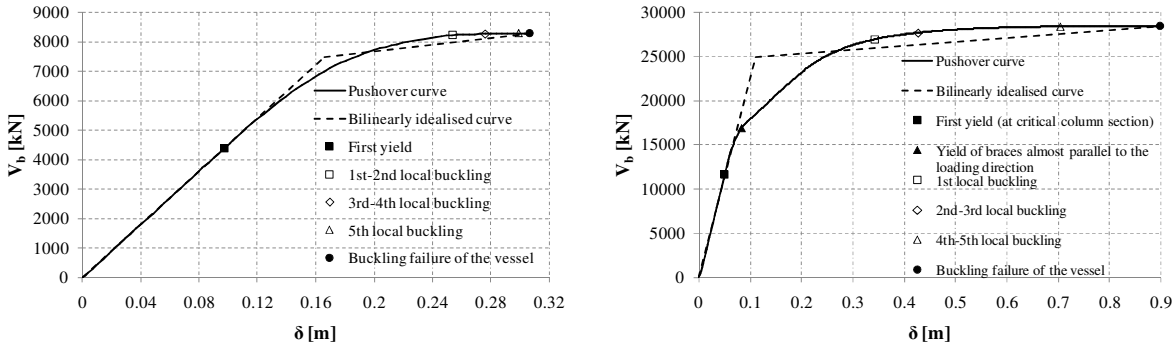

a. AB1 (Moment-resisting LLRS) b. AB2 (Braced LLRS)

Figure 5. Pushover curves of the selected pressure vessels

For vessel AB1 its response is initially elastic until the first yield. Then, critical sections at the top of the columns yield one by one until those at the columns with the maximum compression buckle locally a little after their yielding (class 3 sections) resulting to the buckling failure of the pressure vessel. For vessel AB2 the response remains practically elastic until the yielding of braces which are almost parallel to the loading direction, where a significant drop in the horizontal stiffness of the vessel takes place. After this point, the yielding of critical column sections continues until they fail due to local buckling before they reach their rotational capacity (class 2 sections) resulting again to the buckling failure of the vessel. In comparison to AB1, AB2 has significantly larger stiffness, strength and ductility, something that seems to be attributed mainly to the presence of braces, and less to the better class section for the columns of AB2. In order to verify this observation, two additional models were created; one similar to AB2 but without braces, denoted by EB2, and one similar to PV1 adding the same braces as in AB2, denoted by EB1 (Fig. 8). For these two models pushover curves were derived and they are shown in Fig. 6 superimposed with the pushover curves for the corresponding initial vessels. The comparison of their characteristic parameters, i.e. initial stiffness, strength, ultimate ductility and eigenperiod, is given in Table 3.

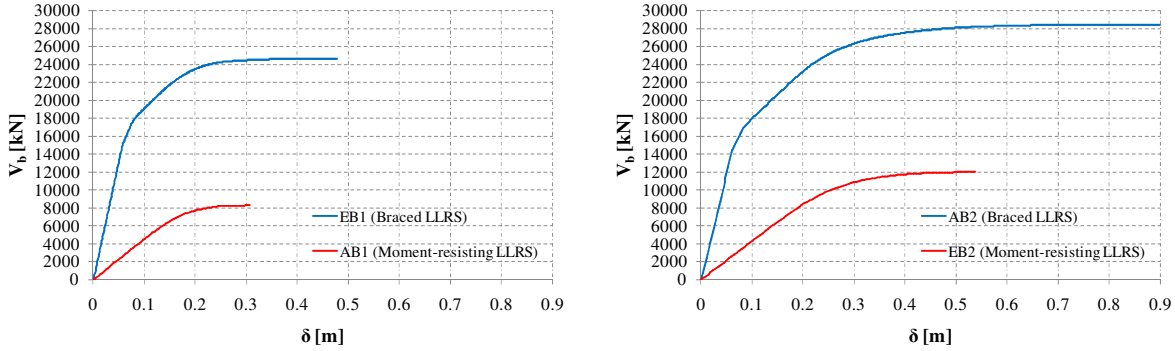

a. Pressure vessel 1 b. Pressure vessel 2

Figure 6. Effect of braces – Pushover curves of spherical pressure vessels AB1, AB2, EB1, EB2

Table 3. Effect of braces – Comparison of characteristic parameters of vessels AB1, AB2, EB1, EB2

Parameter	Pressure vessel 1			Pressure vessel 2		
	AB1	EB1	Difference [%]	EB2	AB2	Difference [%]
Initial stiffness, K [kN/m]	45000	265000	488.9	43000	240000	458.1
Base shear (strength), V_b [kN]	8300	24600	196.4	12000	28000	133.3
Ultimate ductility, μ_u	1.85	5.66	205.9	2.14	8.15	280.8
Eigenperiod, T [sec]	1.53	0.64	-58.2	1.69	0.72	-57.4

From Fig. 6 and Table 3 it is clearly observed in both cases a significant increase in stiffness, strength and ductility and a respectively significant decrease in eigenperiod for the braced lateral load resisting system. Obviously, the overall stiffness and strength of the vessel are increased because the

corresponding stiffness and strength of braces are added to those of the columns. In addition, the increase in stiffness leads to a corresponding decrease in the eigenperiod of the vessel. However, the significant increase in the ultimate displacement and subsequently in ductility is mainly caused by the detailing of the brace-to-column connection (Fig. 7a). More specifically, braces are connected to the column (No. 2) through plate No. 8 and in order to avoid the local failure of the column from the force induced by the brace, three circular plates (Nos. 11 and 32) are placed as stiffeners. Due to these stiffeners the critical section of columns buckles locally according to a higher, hence stiffer, mode (Fig. 7c) compared to an unstiffened column section (Fig. 7b).

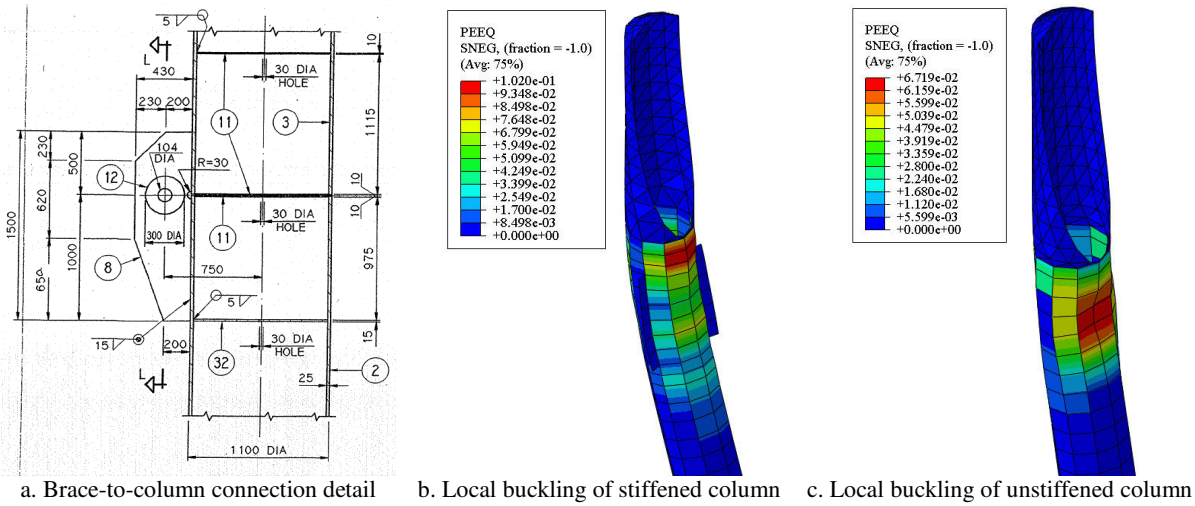

a. Brace-to-column connection detail b. Local buckling of stiffened column c. Local buckling of unstiffened column

Figure 7. Connection of braces at the top of columns and its failure modes

Comparing the two braced (EB1 and AB2) and the two moment-resisting (AB1 and EB2) pressure vessels an increase in stiffness, strength and ductility is observed that seems to be caused solely to their different section classification. In order to investigate that, three additional vessel models denoted by 'ESC' were created for each of the four models with constant column cross sections that belong to class 1, 2 and 3, respectively, changing the section thickness according to the limits for each class given by EC3 (Fig. 8). It is noted that for pressure vessel 1 the two additional models ESC13 and ESC16 with class 3 sections coincide with the vessels AB1 and EB1, respectively. The derived pushover curves are shown in Figs. 9 and 10.

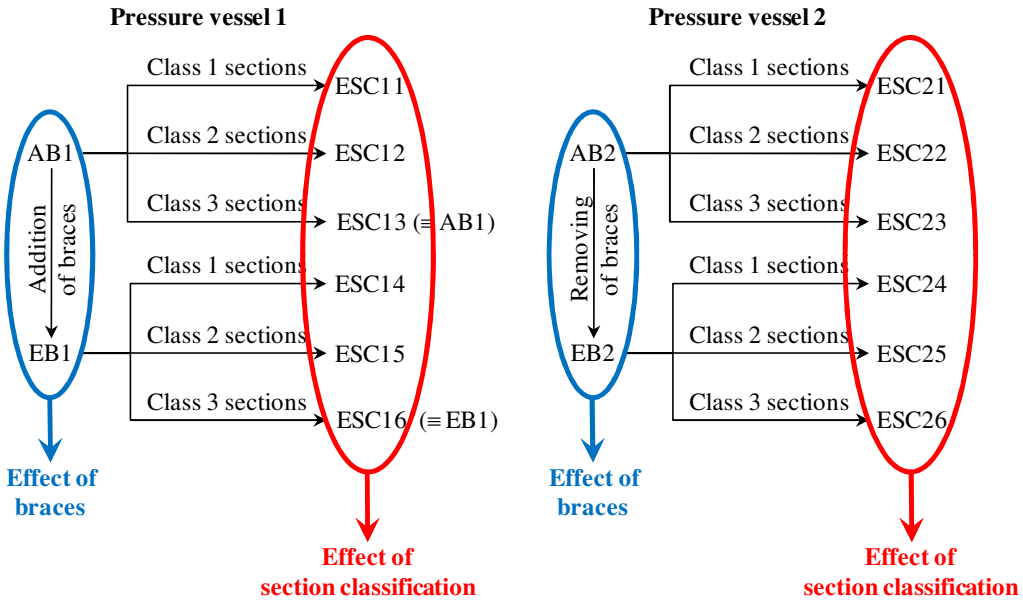

Figure 8. Pressure vessel models used for parametric investigations

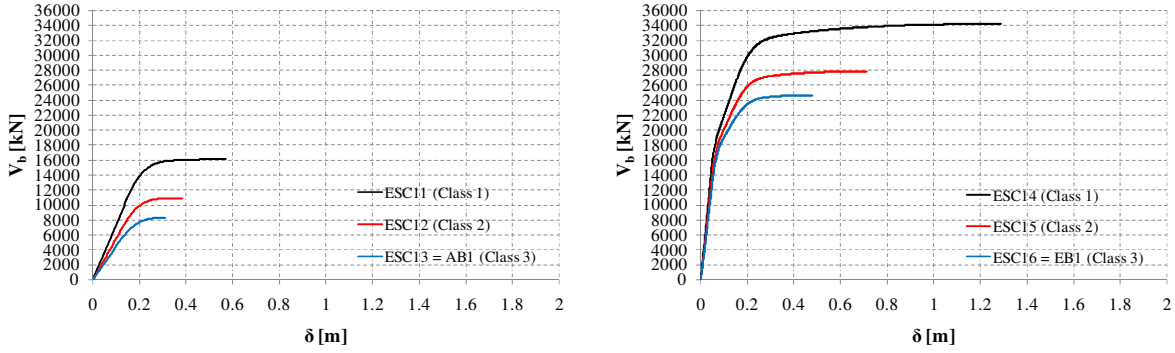

a. Moment-resisting LLRS b. Braced LLRS

Figure 9. Effect of column section class – Pushover curves of spherical pressure vessels ESC11 to ESC16

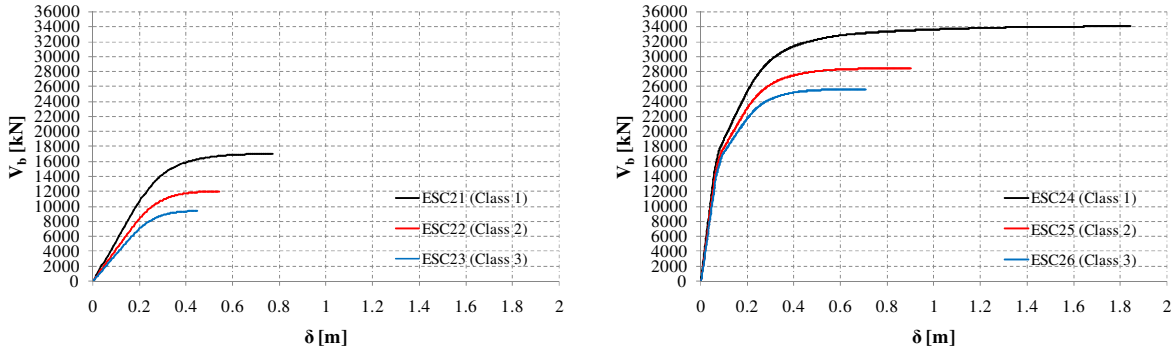

a. Moment-resisting LLRS b. Braced LLRS

Figure 10. Effect of column section class – Pushover curves of spherical pressure vessels ESC21 to ESC26

From the bilinearly idealized curves derived from those of Figs. 9 and 10, it is found that in both cases of class 3 sections for the vessels with braced LLRS the ultimate ductility ($\mu_u=\delta_u/\delta_y$) is 1.85 in ESC16 (≡EB1) and 1.93 in ESC23. Since the corresponding eigenperiods are large (1.53 sec for ESC16 and 1.82 sec for ESC23), the equal displacement approximation holds, thus the behaviour factor for these two cases is equal to the corresponding ultimate ductility. These values are compatible with those suggested in Eurocode 8 (EC8, CEN/TC250/SC8, EN1998-1, 2004) for class 3 sections ($1.5 \le q \le 2.0$).

Furthermore, it is observed that going from class 3 to class 1 sections results in pressure vessels with significantly larger stiffness, strength and ductility and correspondingly smaller eigenperiods. In addition, the difference in percentage terms (Table 4) is larger going from class 2 to class 1 than from class 3 to class 2, reflecting the corresponding increase in the thickness of the column section. More specifically, going from class 3 to class 2 the threshold thickness is increased by 27.7% in vessel case 1 and by 25% in vessel case 2, while from class 2 to class 1 by 43.5% in vessel case 1 and by 40% in vessel case 2.

Table 4. Effect of column section class – % differences of characteristic parameters between the 12 investigated spherical pressure vessels

Parameter	Pressure vessel case 1				Pressure vessel case 2			
	Moment-resisting LLRS		Braced LLRS		Moment-resisting LLRS		Braced LLRS	
	CL3→CL2	CL2→CL1	CL3→CL2	CL2→CL1	CL3→CL2	CL2→CL1	CL3→CL2	CL2→CL1
Initial stiffness, K	23.4	33.3	9.4	12.6	18.1	26.7	7.6	10.3
Base shear (strength), V_b	31.5	47.9	13.0	22.8	28.1	41.8	10.9	19.7
Ultimate ductility, μ_u	14.0	30.3	43.4	42.8	10.4	25.6	18.7	40.5
Eigenperiod, T	- 9.2	- 12.5	- 4.0	- 5.3	- 7.3	- 10.3	- 3.4	- 4.4

Finally, in case of pressure vessels with braces and class 1 sections, the ultimate displacements are extremely high, i.e. 1.29 m for ESC14 and 1.85 m for ESC21. Assuming a typical case for Greece, i.e. EC8 Type 1 elastic spectrum and soil class B, the peak ground acceleration that corresponds to each ultimate displacement is 9.58g and 12.49g, respectively. These extremely high values denote an unrealistically large safety margin, which means that the choice of class 1 column sections in braced systems is not an economically feasible solution.

Having derived the pushover curves for the 14 cases of spherical pressure vessels, one can proceed with the derivation of respective fragility curves. Seven cases have moment-resisting LLRS and the rest braced LLRS. The methodology is applied to all 14 cases and the corresponding damage state threshold values of the peak ground acceleration are derived. Then, in order to derive the representative fragility (probabilistic vulnerability) curves for each of the two pressure vessel categories the sample mean and the sample variance of the seven threshold values of A_g for each damage state are estimated and then, assuming a lognormal probability density function, the corresponding median values of A_g are estimated (Table 5), i.e. the damage state thresholds for each vessel category. The corresponding fragility curves, using a value of β_{tot}=0.55 (as previously described), are plotted in Fig. 11.

Table 5. Damage state threshold values of peak ground acceleration, A_g

Category	DS1 Minor Damage	DS2 Moderate Damage	DS3 Extensive Damage	DS4 Failure/Collapse
Moment-resisting LLRS	0.34	0.60	0.81	1.05
Braced LLRS	0.37	1.74	3.42	5.67

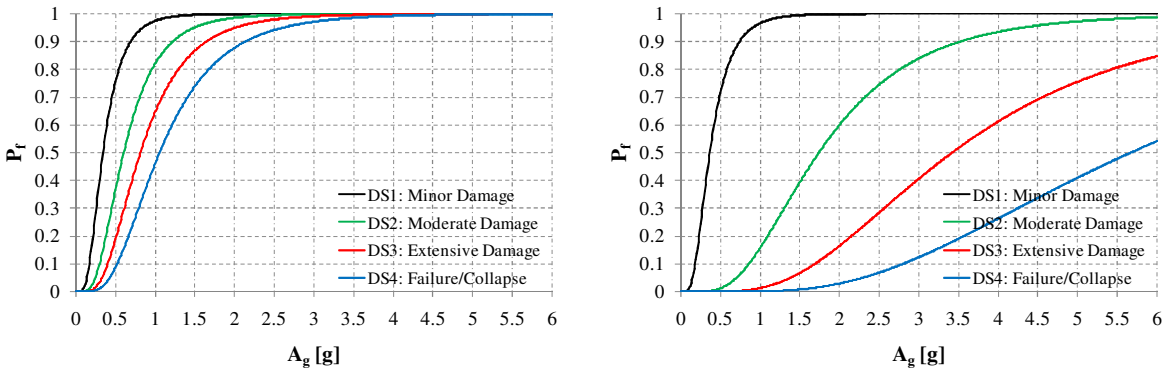

a. Moment-resisting LLRS b. Braced LLRS

Figure 11. Fragility curves for spherical pressure vessels
(H/D=0.60÷0.70, columns pinned at base, class 1, 2 and 3 column sections)

First of all, it is observed that for all damage states the median values of A_g are far larger for pressure vessels with braced LLRS, denoting that the addition of bracings reduce dramatically the fragility of the vessel. Furthermore, it is observed that the difference of the median A_g values between the two vessel categories (with moment-resisting and braced LLRS) increases for the three higher damage states (see Table 5). This means that bracings play a more effective role for increasing levels of damage. Finally, although the medians of the three higher damage states for the pressure vessels with braced LLRS are not realistic, they denote a significant safety margin against high levels of damage caused by the presence of braces.

CONCLUSIONS

In the present study a methodology for the derivation of fragility curves for a 'stock' of spherical pressure vessels is developed based on static nonlinear (pushover) analysis. Damage states are defined on a bilinearly idealised pushover curve taking into account only the damage developed at the

supporting structure and using the vessel displacement as a global damage parameter. The probability density function is considered as having a lognormal distribution.

Two spherical pressure vessels were investigated; one designed without braces (PV1) and one with braces (PV2), concluding that the failure of the both vessels was caused by the local buckling of critical column sections (class 3 and 2, respectively). Then, the effect of braces on the response of spherical pressure vessels was investigated creating two additional pressure vessels, one from PV2 removing the braces and the other from PV1 adding the same braces as those in PV2. It was found that the significant increase to the stiffness (~ 473%), the strength (~ 165%) and the corresponding significant reduction in the eigenperiod (~ 58%) was caused by the addition of the braces, while the significant increase to the ultimate ductility (~ 243%) was caused by the stiffeners placed to columns to form the brace-to-column connections. Finally, for each of these four cases, three additional vessels were created varying the thickness of the column cross section according to the class 1, 2 and 3 limits suggested by Eurocode 3, so as to investigate the effect of section classification on vessel response. It was found that the percent difference in stiffness, strength and ultimate ductility of the spherical pressure vessel is larger going from class 2 to class 1, in proportion with the corresponding percent increase of the column thickness.

The proposed methodology was applied to obtain fragility curves for each of the two pressure vessel categories, i.e. with and without braces, with a 0.60÷0.70 ratio of column height to vessel diameter and columns pinned at their base. It was found that braces reduce the fragility of the spherical pressure vessel and become more effective as the level of damage increases, providing at the same time a respectively significant safety margin.

Finally, it should be noted that in the framework of the present research program, the results of the investigations of the detailed analytical models presented herein will be used to develop properly calibrated simple, cost-efficient and reliable models, which can then be used for the development of fragility curves for various types of pressure vessels with different geometries and material properties.

ACKNOWLEDGEMENTS

The present research effort (research program *"Vulnerability and Risk Assessment for the seismic protection of industrial facilities-RASOR" 2012-2015)* has been co-financed by the European Union (European Social Fund – ESF) and Greek national funds through the Operational Program "Education and Lifelong Learning" of the National Strategic Reference Framework (NSRF) - Research Funding Program: THALES. Investing in knowledge society through the European Social Fund.

REFERENCES

CEN/TC250/SC3, EN 1993-1-1 (2005) Eurocode 3: Design of steel structures - Part 1-1: General rules and rules for buildings, Technical Committee 250 - Structural Eurocodes, Subcommittee 3 - Eurocode 3: Design of steel structures, Comité Européen de Normalisation, Brussels.

CEN/TC250/SC8 (2004) Eurocode 8: Design of structures for earthquake resistance - Part 1: General rules, seismic actions and rules for buildings, Technical Committee 250 - Structural Eurocodes, Subcommittee 8 - Eurocode 8: Earthquake resistance design of structures, EN 1998-1, Comité Européen de Normalisation, Brussels.

Curadelli O (2011) "Seismic reliability of spherical containers retrofitted by means of energy dissipation devices", *Engineering Structures*, 33(9):2662-2667

FEMA-ASCE (2001a) Seismic Fragility Formulations for Water Systems: Part 1 - Guideline, American Lifelines Alliance (FEMA-ASCE Public-Private Partnership), Washington, D.C.

FEMA-ASCE (2001b) Seismic Fragility Formulations for Water Systems: Part 2 - Appendices, American Lifelines Alliance (FEMA-ASCE Public-Private Partnership), Washington, D.C.

FEMA-NIBS (2010) Multi-hazard Loss Estimation Methodology - HAZUS-MH MR5: Earthquake Model Technical Manual, Federal Emergency Management Agency (under a contract with the National Institute of Building Sciences), Washington, D.C.

Karakostas C, Makarios T, Lekidis V, Kappos A (2006) "Evaluation of vulnerability curves for bridges – A case study", *CD-ROM Proceedings of the 1st European Conference on Earthquake Engineering and Seismology – 1st ECEES*, Geneva, Switzerland, September 3-8, Paper No. 1435

Lekidis VA, Karakostas CZ, Sous I, Anastasiadis A, Kappos A, Panagopoulos G (2005) "Evaluation of economic loss for structures in the area struck by the 7/9/1999 Athens earthquake and comparison with actual repair costs", *Proceedings of the 5st International Conference on Earthquake Resistant Structures – ERES2005*, Skiathos, Greece, May 30 – June 1, pp. 310-310

Moschonas IF, Kappos AJ, Panetsos P, Papadopoulos V, Makarios TK, Thanopoulos P (2009) "Seismic fragility curves for greek bridges: methodology and case studies", *Bulletin of Earthquake Engineering*, 7(2):439-468

Moschonas IF and Kappos AJ (2011) "Generalized fragility curves for bearing-supported skew bridges, for arbitrary angle of incidence of the seismic action", *CD-ROM Proceedings of the ECCOMAS Thematic Conference on Computational Methods in Structural Dynamics and Earthquake Engineering - COMPDYN 2011*, Corfu, Greece, May 25-28, Paper No. 377

Tung ATY and Kiremidjian AS (1989) Seismic reliability analysis methods for elevated spherical tanks, Report No. 89, The John A. Blume Earthquake Engineering Center, Department of Civil and Environmental Engineering, Stanford University, CA